Generation of Affibody® ligands binding interleukin-2 receptor α/CD25

Caroline Grönwall*, Eveline Snelders†, Anna Jarelöv Palm‡, Fredrik Eriksson†, Nina Herne‡ and Stefan Ståhl*[1]

**Department of Molecular Biotechnology, School of Biotechnology, AlbaNova University Center, Royal Institute of Technology (KTH), SE-106 91 Stockholm, Sweden, †Department of Oncology and Pathology, Cancer Center Karolinska (CCK), Karolinska Hospital, SE-171 76 Stockholm, Sweden, and ‡Affibody AB, Box 20137, SE-161 02 Bromma, Sweden*

Affibody® molecules specific for human IL-2Rα, the IL-2 (interleukin-2) receptor α subunit, also known as CD25, were selected by phage-display technology from a combinatorial protein library based on the 58-residue Protein A-derived Z domain. The IL-2R system plays a major role in T-cell activation and the regulation of cellular immune responses. Moreover, CD25 has been found to be overexpressed in organ rejections, a number of autoimmune diseases and T-cell malignancies. The phage-display selection using Fc-fused target protein generated 16 unique Affibody® molecules targeting CD25. The two most promising binders were characterized in more detail using biosensor analysis and demonstrated strong and selective binding to CD25. Kinetic biosensor analysis revealed that the two monomeric Affibody® molecules bound to CD25 with apparent affinities of 130 and 240 nM respectively. The Affibody® molecules were, on biosensor analysis, found to compete for the same binding site as the natural ligand IL-2 and the IL-2 blocking monoclonal antibody 2A3. Hence the Affibody® molecules were assumed to have an overlapping binding site with IL-2 and antibodies targeting the IL-2 blocking Tac epitope (for example, the monoclonal antibodies Daclizumab and Basiliximab, both of which have been approved for therapeutic use). Furthermore, immunofluorescence microscopy and flow-cytometric analysis of CD25-expressing cells demonstrated that the selected Affibody® molecules bound to $CD4^+$ $CD25^+$ PMBCs (peripheral-blood mononuclear cells), the IL-2-dependent cell line NK92 and phytohaemagglutinin-activated PMBCs. The potential use of the CD25-binding Affibody® molecules as targeting agents for medical imaging and for therapeutic applications is discussed.

Introduction

IL-2 (interleukin 2) and its corresponding receptor (IL-2R) are important in T-cell activation and regulation of cellular immune responses. The IL-2R is one of the most extensively studied cytokine receptor complexes and comprises the α subunit (IL-2Rα), the β subunit (IL-2Rβ) and the common cytokine γ subunit (IL-2Rγ_c) [1]. IL-2 signalling is initiated by ligand-induced assembly of the receptor complex, resulting in activation of multiple signalling pathways [2]. The IL-2Rα subunit, also known as CD25 and originally identified as the Tac antigen, is a specific receptor for IL-2 and plays a critical role in signalling and activation of cells. This is despite the fact that the 55 kDa cell-surface-expressed glycoprotein has a very short cytoplasmic tail and no signal-transduction capacity [3,4]. CD25 alone is also termed the 'low-affinity' IL-2R, binding to IL-2 with an affinity of 10 nM [5]. Interaction of IL-2 with CD25 has been suggested to induce receptor oligomerization, including the sequential recruitment of the IL-2Rβ and IL-2Rγ_c chains and formation of the high-affinity three-receptor complex ($K_D \sim 10$ pM) [4,6].

The CD25 receptor is not expressed on resting T-cells, and only less than 5% of all normal PBMCs (peripheral-blood mononuclear cells) express CD25 and then at low levels. However, upon activation, the expression of CD25 is rapidly up-regulated [7]. Moreover, as part of the cytokine regulatory system, CD25 can be shed from the surface of expressing cells, and the release of the soluble form of CD25 is proportional to the level of cell-surface expression [7]. CD25 has, in addition, proved to be an important marker for defining the regulatory T-cell population ($CD4^+$,

Key words: Affibody® molecule, interleukin-2 receptor α (IL-2Rα/CD25), phage display, peripheral-blood mononuclear cell (PBMC), protein engineering.

Abbreviations used: ABD, albumin-binding domain; BIA, biospecific interaction analysis; CD25, interleukin-2 receptor α; DAPI, 4′,6-diamidino-2-phenylindole; DMEM, Dulbecco's modified Eagle's medium; DTT, dithiothreitol; HSA, human serum albumin; HI FBS, heat-inactivated fetal bovine serum; His_6, hexahistidine; HRP, horseradish peroxidase; IL-2, interleukin 2; IL-2Rα, interleukin-2 receptor α (CD25); IMAC, immobilized-metal-ion affinity chromatography; mAb, monoclonal antibody; o/n, overnight; OG, Oregon Green® 488 maleimide; PBMC, peripheral-blood mononuclear cell; PEG, poly(ethylene glycol); PEST, 100 units/ml penicillin plus 100 μg/ml streptomycin; pfu, plaque-forming unit; PHA, phytohaemagglutinin; RT, room temperature; TSB, tryptic soy broth; TYE, tryptone/yeast extract.

[1] To who correspondence should be addressed (stefan.stahl@biotech.kth.se).

$CD25^+$ and $FOXP3^+$) [8]. Regulatory T-cells are a small subset of the T-cell population that has been suggested to contribute to suppression of autoimmune responses and maintaining balance of the immune system, as well as play a presumably important role in antitumour immunity [8–10]. CD25 has been found to be significantly overexpressed on cells involved in different inflammatory autoimmune diseases, organ-transplant rejections and in a variety of T-cell malignancies [7,11]. Hence CD25 has been demonstrated to be a uniquely valuable target for immunotherapy and for understanding the underlying mechanisms of the IL-2R system in relation to disorders of the immune system. Furthermore, since CD25 is expressed only in activated immune cells, the future use of agents targeting CD25 could also be considered in the field of medical imaging. *In vivo*, CD25 targeting could potentially be used for the visualization of inflammation in autoimmune diseases and for exploring infiltration of active immune cells in solid tumours, in order to monitor and improve therapy.

Antibodies are excellent agents for targeting therapeutically interesting proteins, since they have naturally evolved to recognize their target and to bind specifically and with high affinity. Several mAbs (monoclonal antibodies) against CD25 have been developed for diagnostic and therapeutic purposes. One example is the therapeutic humanized antibody daclizumab, targeting CD25 and blocking IL-2 binding, approved for therapeutic treatment to prevent organ rejection in kidney transplantation and showing promising results in the treatment of T-cell leukaemia and autoimmune diseases such as T-cell mediated uveitis and multiple sclerosis [12].

Antibodies offer many promising features as targeting agents. However, in medical imaging and radionuclide-based diagnostics, their large size will be disadvantageous, leading to slow clearance and thus a higher background signal. This has led to the development of smaller antibody fragments [13], such as Fab [14], Fv [15], single chain Fv [16,17], diabody [18] and single-domain antibodies [19,20]. Rather recently, these various antibody approaches have been complemented with efforts based on protein scaffolds [21–25], including trinectins [26,27], anticalins [28], designed ankyrin repeat proteins [29], PDZ (postsynaptic density protein, *Drosophila* disc large tumour suppressor and zonula occludens-1 protein) domains [30] and Affibody® (Affibody® AB, Bromma, Sweden) molecules [31]. Initially, these engineered protein domains were investigated for a range of biotechnological applications, but different therapeutic and molecular-imaging approaches have recently become a focus of research.

Affibody® molecules [32] are based on a 58-amino-acid-residue protein domain derived from the IgG-binding domains from staphylococcal protein A. This cysteine-free three-helix bundle domain, designated the 'Z domain' [33], has been used as a scaffold for construction of combinatorial libraries from which target-specific Affibody® variants can be selected with affinities down to picomolar levels. Affibody® molecules have shown potential in a wide variety of different applications, such as in bioseparations [34–36], as detection reagents [37–40], in the inhibition of receptor interactions [41], for depletion in proteomics research [42] and for tumour targeting applications [43–50]. The high stability, low-molecular-mass ($\sim$6.5 kDa), high production efficiency in *Escherichia coli* and the possibility for straightforward thiol-based directed coupling or labelling, are favourable features in comparison with those of other affinity ligands [23]. The Affibody® molecules have, in addition, been demonstrated to be conveniently produced by either recombinant means in bacteria or by chemical synthesis [51].

Consequently, the Affibody® molecules have the potential to be suitable as therapeutic or imaging agents targeting CD25. There are several interesting fields of possible application for an anti-CD25 Affibody® ligand, the three most promising being:

(i) therapeutic treatment in prevention of organ rejection or autoimmune disease
(ii) medical imaging to visualize active immune cells in inflammatory responses, autoimmune diseases or in tumours
(iii) therapeutic depletion of $CD25^+$ cells in T-cell leukaemia.

The Affibody® molecules are very flexible in their usability. The same Affibody® molecule can easily be labelled for different detection systems, fused to different therapeutic effector groups or coupled to a fusion partner to alter its circulation half-life in order to make it suitable for different applications [23,47,48].

In the present study we describe the selection and initial characterization of Affibody® molecules binding to human IL-2Rα/CD25. The novel Affibody® ligands were selected using on Fc-fused target protein and phage-display technology. Binding of the selected Affibody® molecules to the extracellular domain of CD25 was characterized with biosensor methods and binding properties, including specificity and affinity, were determined. Moreover, a competitive biosensor assay was used for an investigation into whether the Affibody® binding epitope on CD25 overlaps the binding site of the natural ligand IL-2. The Affibody® molecules were further evaluated for binding to native CD25 expressed on activated and non-activated $CD25^+$ PBMCs and the human IL-2-dependent cell line NK92. The potential use of CD25-binding Affibody® molecules for medical imaging of inflammation and for diagnostic and therapeutic applications is discussed.

Materials and methods

Strains, vectors and phagemid library

The amber suppressor *E. coli* strain RR1ΔM15 [52] was used as bacterial host for phage production and the cloning procedure. The phagemid vector pAffi1 and the construction of the phagemid library used in the present study, Zlib2002 (3×10^9 members), has been described elsewhere [53]. Two expression vectors were used for subcloning and expression of phagemid inserts from selected clones (pAY01448 and pAY01449) containing a T7 promotor [54] and a multiple cloning site, together with a kanamycin-resistance gene. Moreover, both expression vectors encode an N-terminal His_6 (hexahistidine) tag for affinity purification and, in addition, the plasmid pAY1449 encodes a C-terminal cysteine residue for direct labelling and coupling. The *E. coli* strain BL21(DE3) (Novagen, Madison, WI, U.S.A.) was used for protein production from the pAY1448 and pAY1449 plasmids.

Preparation of phage stocks

Preparation of phage stocks from the library (a portion of Zlib2002) and between selections was performed as described previously [31,55] using the helper phage M13K07 (New England Biolabs, Beverly, MA, U.S.A.). PEG [poly(ethylene glycol)]/NaCl was used for phage precipitation, routinely yielding phage titres of approx. 10^{13} pfu (plaque-forming units)/ml.

Phage selection

Recombinant human IL-2Rα fused to the Fc part of human IgG_1 (CD25–Fc; R&D systems, Minneapolis, MN, U.S.A.) was used as the target protein during phage-display selections and streptavidin-coated paramagnetic beads (Dynabeads® M280 streptavidin; Dynal A.S., Oslo, Norway) with captured biotinylated anti-IgG Affibody® molecule were used as the solid support. The anti-IgG Affibody® molecule is a head-to-tail dimer of the engineered Protein A domain Z [33], hereinafter denoted 'Z_2', site-specifically biotinylated via a C-terminal cysteine residue (Z_2–Cys–biotin). Furthermore, for comparison, a parallel selection using Protein A-precoated paramagnetic beads (Dynabeads®) instead of anti-IgG Affibody® beads was carried out. Four rounds of panning were performed as follows. All tubes and beads were blocked with 5% TPBSB [PBS containing 0.1% Tween 20, 0.02% sodium azide and 5% (w/v) BSA] to avoid non-specific binding. To further remove unwanted Fc binders, streptavidin, anti-IgG Affibody® molecule or Protein A, one round of negative selection was performed before each round of panning. Biotinylated anti-IgG Affibody® protein was allowed to bind to streptavidin beads (15 μg of Affibody® protein/mg of beads) at RT (room temperature; 22 °C) for 30 min with end-over-end rotation to generate anti-IgG Affibody®-coated paramagnetic beads. For the negative selections this was followed by capture of human polyclonal Fcγ (Jackson ImmunoResearch Laboratories, West Grove, PA, U.S.A.; 4 μg of Fc/mg of beads) at RT for 1 h with continuous rotation. The phage stock was then preadsorbed on the Fc-coated anti-IgG Affibody® beads for 1 h at RT and the supernatant was used as the input in the selection round. For the Protein A-bead selection strategy, negative selection was performed correspondingly and the input phage was preadsorbed on Fc-coated Protein A beads before each selection round. The selections were carried out in solution by mixing phage and target protein in a total volume of 1 ml of 3% TPBSB (as described above, but with 3% BSA). The final concentration of CD25–Fc was 100 nM in selection round 1, 50 nM in round 2, 20 nM in round 3 and 10 nM in round 4.

The selection mixture was incubated for 2 h at RT with continuous rotation. Thereafter the samples were transferred to blocked anti-IgG Affibody® beads, and incubated for 20 min to capture the phage–CD25 complex. The amount of beads was decreased twice for each round, starting with 1 mg of beads in round 1. The beads with bound binders were washed for 3 min per wash with increasing stringency for each round by increasing the number of washes (three times in round 1, five times in round 2 and seven times in rounds 3 and 4) and the amount of Tween 20 in the wash buffer (0.1% Tween 20 in round 1 and 0.5% Tween 20 in the following rounds). As washing buffer, 3% TPBSB was used in all steps except the last wash, where PBS (10 mM phosphate/150 mM NaCl, pH 7.2) was used. Bound phage was eluted with 500 μl of 50 mM glycine/HCl, pH 2.1, for 10 min at RT, followed by immediate neutralization with 50 μl of 1 M Tris/HCl, pH 8.0, and 450 μl of PBS. Eluted phage was used to infect RR1ΔM15 cells in exponential growth phase. The infected cell suspensions were spread on TYE (tryptone/yeast extract)/agar plates supplemented with 2% (w/v) glucose and 100 mg/l ampicillin, and incubated o/n (overnight) at 37 °C. The colonies were thereafter collected by resuspension in TSB (tryptic soy broth) culture medium supplemented with 0.5% yeast extract, and a fraction was used for the amplification of phage, generating a new phage library. Phagemid particles were rescued from infected cells using the helper phage M13K07, purified and concentrated by PEG precipitation. The selection process was monitored by titration of the phage stocks before selection and after elution. A serial dilution of phage solutions were allowed to infect exponential-phase RR1ΔM15 cells, spread on TYE plates and incubated o/n at 37 °C.

ELISA for post-selection screening

Affibody® proteins from clones obtained after four rounds of selection were produced in 96-well plates and analysed

for their CD25-binding activity using an ELISA. Randomly picked colonies (93 clones from selection round 3 and 465 clones from selection round 4) were separately inoculated in 1 ml of TSB medium supplemented with 0.5% yeast extract, 100 mg/l ampicillin (Tamro, Vantaa, Finland) and 1 mM isopropyl β-D-thiogalactoside (Apollo Scientific, Bredbury, Stockport, Cheshire, U.K.) in deep-well plates and grown with shaking o/n at 37°C. Thus Affibody® proteins from the individual clones were expressed directly from the pAffi1 phagemid vector as fusion proteins with an ABD (albumin-binding domain) [56]. Cells were pelleted by centrifugation at 3000 ***g*** for 10 min, the supernatant was discarded and the cell pellets were resuspended in 400 μl of PBS containing 0.05% Tween 20. The cells were disrupted by freezing at −80°C, followed by thawing in a water bath. Centrifugation at 3500 ***g*** for 20 min resulted in pelleted insoluble material and the Affibody® proteins in the supernatant. In the ELISA assay, 96-well half-area plates (Corning, Lowell, MA, U.S.A.) were coated with HSA (human serum albumin) (Sigma–Aldrich, Steinheim, Germany), 6 μg/ml in 50 mM sodium carbonate, pH 9.5, per well o/n at 4°C. After blocking the plates with 2% (w/v) low-fat dried skimmed milk powder in PBS/0.05% Tween 20, the crude protein supernatants were added and the plates were incubated for 1.5 h at RT with shaking. The CD25-binding activity was detected by incubation with CD25-Fc (1 μg/ml; R&D systems), followed by incubation with HRP (horseradish peroxidase)-conjugated anti-(human IgG Fc) antibody (1:4000; Dako, Glostrup, Denmark) and visualization with ImmunoPure® TMB (3,3',5,5'-tetramethylbenzidine) substrate (Pierce, Rockford, IL, U.S.A.). Furthermore, an ELISA for detection of unwanted binders to the Fc part of the fusion protein was performed in parallel, following the same experimental set-up as described above, but replacing the target protein with human polyclonal Fc (1 μg/ml; Jackson ImmunoResearch Laboratories).

DNA sequencing and sequence clustering

DNA sequencing of phagemid (pAffi1) inserts was performed after four rounds of panning on clones that were found to be positive when screened in ELISA. Altogether 101 positive clones were chosen and sequenced on an ABI Prism® 3100 Genetic Analyzer (Applied Biosystems, Foster City, CA, U.S.A.). Furthermore, the unique amino acid sequences of the Affibody® molecules from the CD25 selection obtained were analysed for sequence similarities using an in-house-developed cluster analysis tool based on so-called 'average-link hierarchal clustering', which has been described in more detail by Orlova et al. [46].

DNA constructions

DNA fragments encoding five different potentially CD25-binding Affibody® molecules ($Z_{CD25:2015}$, $Z_{CD25:2018}$, $Z_{CD25:2020}$, $Z_{CD25:2021}$ and $Z_{CD25:2022}$) were subcloned from the pAffi1 phagemid as monomers into the expression vector pAY01448. Correct clones were verified by using PCR screening and DNA sequencing. The two 'best' CD25-binding Affibody® molecules, namely $Z_{CD25:2015}$ and $Z_{CD25:2020}$, were further subcloned as head-to-tail dimers into the expression vectors pAY01448 and pAY01449, giving dimeric proteins of the two Affibody® molecules with and without a C-terminal cysteine residue.

Expression and purification of His_6-tag fusion proteins

Five different Affibody® proteins ($Z_{CD25:2015}$, $Z_{CD25:2018}$, $Z_{CD25:2020}$, $Z_{CD25:2021}$ and $Z_{CD25:2022}$) from the CD25 phage display selection were expressed in the *E. coli* strain BL21(DE3) from the pAY01448 vector, thus generating monomeric His_6-fusion proteins. The CD25-binding Affibody® molecules $Z_{CD25:2015}$ and $Z_{CD25:2020}$ were, in addition, expressed as head-to-tail dimers from the expression vectors pAY01448 and pAY01449, giving His_6-tagged Affibody® dimers with and without a C-terminal cysteine residue. The His_6-fusion proteins were expressed as described previously [53] and purified using IMAC (immobilized-metal-ion affinity chromatography) purification on His GraviTrap™ columns (GE Healthcare, Uppsala, Sweden) under denaturing conditions according to the manufacturer's recommendations. Buffer exchange was performed using PD10™ columns (GE Healthcare) and the proteins were stored in PBS. The purity of the protein preparations was assessed by SDS/PAGE, and the protein concentrations were determined with A_{280} measurements using appropriate specific absorption coefficients.

Biosensor analysis

A Biacore® (GE Healthcare) 2000 instrument was used for real-time BIA (biospecific interaction analysis) between selected Affibody® molecules and CD25. In the first affinity screening, five different Affibody® variants from the CD25 phage display selection (His_6-$Z_{CD25:2015}$, His_6-$Z_{CD25:2018}$, His_6-$Z_{CD25:2020}$, His_6-$Z_{CD25:2021}$, His_6-$Z_{CD25:2022}$) were analysed for binding to CD25. Recombinant human IL-2Rα (CD25; R&D systems) was immobilized by amine coupling on to the dextran layer of a CM5 chip according to the manufacturer's instructions. For comparison and to serve as controls, the Fc fused CD25, CD25–Fc (R&D systems) and an irrelevant Fc-fused protein, CD33–Fc (R&D systems), were separately immobilized on two chip surfaces. The Affibody® proteins were diluted in HBS-EP buffer (5 mM Hepes, 150 mM NaCl, 3.4 mM EDTA and 0.005% surfactant P20, pH 7.4) to a final concentration of 1 μM and injected at a constant flow rate of 30 μl/min.

To ensure that the immobilization of CD25 did not influence the binding to the Affibody® molecules, a control

experiment was performed using a CM5 chip biosensor surface coupled with Protein A according to the manufacturer's instructions. CD25–Fc was injected over the Protein A surface, directly followed by injection of an anti-CD25 Affibody® ligand without any regeneration between the two injections. In this experimental set-up, the CD25–Fc protein will be coupled to the surface in a directed manner via the Fc part, presumably without affecting the binding properties of CD25.

The CD25 interaction of the two best CD25 binders from the initial Biacore® ranking, $Z_{CD25:2015}$ and $Z_{CD25:2020}$, were further characterized in more detail as follows. First, the monomeric Affibody® molecules were subjected to kinetic analysis, in which His_6-$Z_{CD25:2015}$ and His_6-$Z_{CD25:2020}$ were injected over a CD25 surface [~1100 RU (resonance units) immobilized by amine coupling] in concentrations ranging from 5 to 640 nM, with a flow rate of 50 μl/min. The dissociation equilibrium constant (K_D) was estimated using the BIAevaluation 3.2 software (Biacore). Furthermore, the binding profiles of the monomeric Affibody® molecules (His_6-$Z_{CD25:2015}$ and His_6-$Z_{CD25:2020}$) were compared with the head-to-tail dimers [His_6-$(Z_{CD25:2015})_2$ and His_6-$(Z_{CD25:2020})_2$] and with the natural CD25 ligand IL-2 by subsequently injecting the analytes at 50 nM over the CD25 surface.

Secondly, dimeric Affibody® molecules, His_6-$(Z_{CD25:2015})_2$-Cys and His_6-$(Z_{CD25:2020})_2$-Cys, were separately immobilized by thiol coupling on to the carboxylated dextran layer of a CM5 chip, according to the manufacturer's recommendations. In order to study the specificity of the Affibody® molecules towards CD25, the following proteins were injected over the Affibody® surfaces at a concentration of 3 μg/ml: CD25–Fc (R&D systems), HSA (Sigma), human IgG (Sigma), human polyclonal IgG Fc (Jackson ImmunoResearch Laboratories), human transferrin (Sigma), human haemopexin [RDI (Research Diagnostics Inc. Division of Fitzgerald Industries International), Concord, MA, U.S.A.], human fibrinogen (Sigma), human IgA (Sigma), human complement C4 (RDI) and streptavidin (Pierce). In addition, the ability of the Affibody® molecules to bind to the murine variant of CD25 was studied by injection of 0.1 and 1 μM recombinant mouse IL-2Rα (R&D systems) over the Affibody®-coupled biosensor surfaces.

Moreover, the binding sites of the Affibody® molecules $Z_{CD25:2015}$ and $Z_{CD25:2020}$ on CD25 were investigated by competition studies with IL-2 and mAbs in the Biacore® instrument. In an initial experiment, competition between the two Affibody® molecules for the same CD25 epitope was evaluated. Equal amounts of CD25–Fc (100 nM) were mixed with two different concentrations of the dimeric Affibody® molecule His_6-$(Z_{CD25:2015})_2$ (10 and 100 nM) and injected over the $Z_{CD25:2020}$-coupled surface (as described above) and the response was compared with that of pure CD25–Fc (100 nM). Similarly, competition with the natural ligand of CD25, IL-2, was studied by mixing CD25–Fc (50 nM) with different concentrations of human recombinant IL-2 (R&D systems) ranging from 5 to 500 nM before injection over the $Z_{CD25:2020}$ surface. In another approach to determine the binding region for the Affibody® molecules as a confirmation of the IL-2 competition study, competition with three mAbs was studied. The anti-CD25 antibodies, namely mAb ON94 (1 μg/ml; Abcam, Cambridge, U.K.), binding in the region of amino acids 3–104, mAb 2A3 (0.5 μg/ml; BD Biosciences, San Jose, CA, U.S.A.), binding the Tac epitope, also referred to as 'epitope A' and competing with IL-2 and mAb M-A251 (M-A251-FITC, 1.3 μg/ml; BD Biosciences), binding epitope B distinct from epitope A, were separately injected directly after CD25–Fc injections over the anti-CD25 Affibody® $Z_{CD25:2020}$ surface using the command co-inject. Injections of HBS-EP buffer and IL-2 (0.8 μg/ml) performed in the same manner were used as controls.

For all Biacore® experiments, the surfaces were regenerated with 10 mM HCl after each injection. One surface on the chips in the different experimental set-ups was activated and de-activated and used as a reference. The response from the reference surface was subtracted from all curves when evaluating the results.

Fluorophore labelling

The anti-CD25 Affibody® molecule His_6-$(Z_{CD25:2020})_2$-Cys and the negative control Affibody® molecule His_6-$(Z_{A\beta:1170})_2$-Cys (binding to amyloid β-peptide [53]) were labelled in a directed manner to the unique C-terminal cysteine residue with OG (Oregon Green® 488 maleimide) (Molecular Probes, Leiden, The Netherlands). The Affibody® proteins, 500 μg in PBS, were reduced using 20 mM DTT (dithiothreitol) at 37 °C for 45 min. Thereafter, the excess DTT was removed on a NAP™-5 column (GE Healthcare), followed by addition of a 10 mM solution of OG to the proteins at a 20-fold molar excess and incubation in the dark for 2 h at RT. Buffer exchange was performed by extensive dialysis against PBS using Slide-A-Lyzer dialysis cassettes (molecular-mass cut-off 3500 Da; volume 0.5–3 ml; Pierce) to remove excess fluorophore.

Cells and cell culture

The human IL-2-dependent cell line NK92 (kindly provided by Dr Siraç Dilber, Division of Hematology, Department of Medicine, Karolinska Institute, Stockholm, Sweden) was used for immunofluorescence-microscopic and flow-cytometric analysis. The cells were maintained in RPMI 1640 medium (Invitrogen) supplemented with 20% (v/v) HI FBS (heat-inactivated fetal bovine serum; Invitrogen), 2 mM L-glutamine (Invitrogen), 2.5 μg/ml amphotericin B (Invitrogen), PEST (100 units/ml penicillin plus 100 μg/ml streptomycin) (Invitrogen) and 100 i.u/ml IL-2 (Proleukin;

Chion Healthcare, Suresnes, France). The cells were maintained at 37 °C in an incubator with humidified air equilibrated with 5% CO_2. PMBCs for immunofluorescence-microscopic and flow-cytometric studies were isolated from healthy blood donors by density-gradient centrifugation using Ficoll-Paque PLUS gradient (GE healthcare) according to the manufacturer's instructions. The cells obtained were washed twice with DMEM (Dulbecco's modified Eagle's medium) (Invitrogen) supplemented with 10 mM Hepes, 25 μg/ml gentamycin, 50 μM 2-mercaptoethanol and 1% HI FBS and $CD25^+$ cells were magnetically separated using the $CD4^+$ $CD25^+$ Regulatory T Cell Isolation Kit (Miltenyi Biotec, Bergisch-Gradbach, Germany). $CD4^+$ $CD25^-$ cells were also collected from this procedure and used as negative control. Flow-cytometric analysis was additionally performed with PHA (phytohaemagglutinin)-activated PBMCs. PBMCs were isolated, with informed consent, from healthy blood donors using Ficoll-Paque MEDIUM gradient (GE healthcare) according to the manufacturer's instructions, and cells were cultured in RPMI 1640 medium (Invitrogen) supplemented with 10% fetal bovine serum (Invitrogen), 10 mM Hepes (Invitrogen), PEST and 5 μg/ml PHA-L (a tetramer of L-type subunits; Sigma) for 66 h at 37 °C with 5% CO_2 to induce activation and CD25 expression. The cells with high CD25 expression were thereafter magnetically isolated with CD25 Dynabeads (Dynal, Oslo, Norway) and the beads were detached from the cells before analysis with DETACHaBEAD (Dynal).

Immunofluorescence microscopy

Immunofluorescence was studied for the dimeric anti-CD25 Affibody® molecule $(Z_{CD25:2020})_2$ binding to NK92 cells and $CD25^+$ PBMCs. Slides were prepared by cytocentrifugation of 200 μl of an NK92-cell or PBMC suspension [2.5×10^5 cells/ml at 220 ***g*** for 5 min in a Shandon Southern Instruments (Sewickley, PA, U.S.A.) Cytospin 1 cytocentrifuge]. Cells were fixed with 3% (v/v) formaldehyde in PBS for 10 min, followed by blocking with 1% BSA/1% fetal bovine serum in PBS. Thereafter, cells were stained for CD25 expression by incubation with the OG-conjugated Affibody® molecule His_6-$(Z_{CD25:2020})_2$-Cys-OG (5 μg/ml) at RT in a dark moist chamber for 30 min. The slides were washed twice with PBS and mounted using VECTASHIELD mounting medium (Vector Laboratories, Burlingame, CA, U.S.A.). Fluorescence was analysed using a Zeiss Axioplan 2 microscope, and images were collected with an AxioCam HRm camera and Axiovision 4.2 software (Zeiss Inc., Göttingen, Germany). OG-conjugated amyloid β-peptide-binding Affibody® molecule [His_6-$(Z_{A\beta:1170})_2$-Cys-OG] was used as a negative control for the Affibody® staining, and $CD25^-$ PMBCs were used as control cells, following the protocol described above.

Flow cytometry

Binding of the dimeric CD25-binding Affibody® molecule $(Z_{CD25:2020})_2$ to NK92 cells and $CD4^+$ $CD25^+$ PBMCs was analysed by flow cytometry using a FACSCalibur instrument (BD Biosciences). Single cell suspensions were prepared and the cells were stained in PBS supplemented with 1% BSA with 5 μg/ml OG-conjugated Affibody® dimer [His_6-$(Z_{CD25:2020})_2$-Cys-OG] for 30 min at 4 °C, followed by washing and resuspension in PBS. OG-conjugated amyloid β-peptide-binding Affibody® molecule [His_6-$(Z_{A\beta:1170})_2$-Cys] and $CD25^-$ PBMCs ($CD4^+CD25^-$) were used as negative controls. Flow-cytometric data were analysed with CELLQuestPro software (BD Biosciences), 10000 events being recorded. Expression of CD25 was verified using FITC-conjugated mAb M-A251 (BD Biosciences). In addition, flow-cytometric analysis was performed with a monomeric Affibody® molecule on PHA-stimulated PMBCs using a FACS Canto II (BD Biosciences) instrument. The PHA-stimulated cells isolated using CD25 beads were washed twice in PBS supplemented with 1% BSA and incubated with 10 μg/ml $Z_{CD25:2020}$ at 4 °C for 1 h. Binding of the Affibody® molecule was visualized with a goat anti-(Affibody® antibody) (Affibody® AB) and Alexa 647®-conjugated anti-goat antibody (Molecular Probes). Furthermore, the mAb ON94 (Abcam) was used as a positive control and the amyloid β-peptide-binding Affibody® His_6-$(Z_{A\beta:1170})_2$ was used as a negative control. Acquisition of flow-cytometric data was performed using BD FACSDiva 5.0.1 software (BD Biosciences), 10000 events being recorded. Data was analysed with Winlist 6.0 software (Verity Software House, Topsham, ME, U.S.A.).

Results

Phage selections of CD25-binding Affibody® molecules

CD25 (IL-2Rα)-specific Affibody® molecules were isolated from a combinatory protein library using phage display *in vitro* selection technology. Four rounds of panning were performed using Fc-fused CD25 (CD25–Fc) as the target protein and paramagnetic beads for in-solution capture of phage, taking advantage of the Fc–Protein A interaction. Two different paramagnetic beads were evaluated, i.e. streptavidin beads coated with a biotinylated dimeric form of an engineered IgG-binding domain of Protein A denoted Z_2 (anti-IgG Affibody® beads) and precoated Protein A (five IgG-binding domains) beads. Monitoring the phage titres during selection revealed that the percentage of eluted phage compared with input phage increased with each round, as expected, implying that target-binding phages were amplified in the selection procedure (Figure 1A). As a confirmation, we also monitored the phage titres in the last wash before

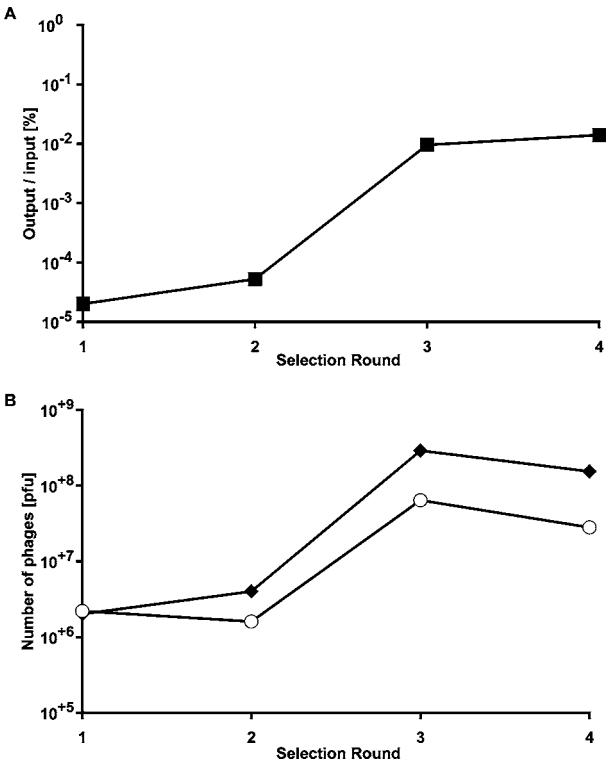

Figure 1 Monitoring the phage titres in the phage-display selection of Affibody® molecules binding to Fc-fused CD25 using capture with Z_2-coated magnetic beads

(**A**) Fraction of phage out (output) compared with the fraction of phage in (input) [output/input (%)] for each selection round. (**B**) The absolute numbers of eluted phage (◆) compared with the absolute numbers of phage in the last washing step (○) in each selection round.

elution: increasingly more phage in the eluate compared with the last wash was shown in every selection round (Figure 1B).

After the fourth round of panning, resulting clones expressing Affibody® molecules were screened using an ELISA for CD25-binding activity. The ELISA showed that approx. 42% of the clones from the anti-IgG Affibody® (Z_2) bead selection (Figure 2) compared with only 8% of the clones from the Protein A bead selection (results not shown) seemed to bind CD25. Selection using somewhat less stringent conditions with higher concentrations of target protein in rounds 3 and 4 (50 nM in both rounds instead of 20 and 10 nM) with anti-IgG Affibody® beads as solid support gave 35% positive clones in round 4, thus showing a slight decrease in the level of positive clones compared with the more stringent selection (results not shown). Screening for binding to Fc showed no specific binding activity towards the Fc part of the target fusion protein for either the Z_2 or the Protein A bead selection, indicating that the negative selection towards Fc had been successful in excluding undesired Fc binders. Interestingly,

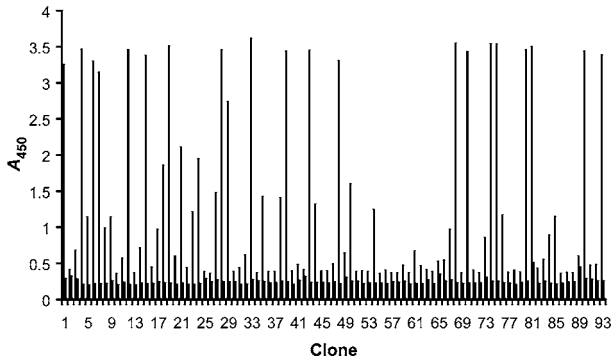

Figure 2 ELISA screening after four rounds of phage-display selection of CD25-binding Affibody® molecules using Fc-fused target protein and capture on Z_2-coated magnetic beads

Affibody® protein from 93 randomly picked clones were individually produced and screened for CD25 binding activity (black bars). The Affibody® molecules from the phage selection were fused to an ABD and captured in microtitre wells coated with HSA. HRP-conjugated anti-(human IgG Fc) antibody was used for detection of binding to CD25–Fc. A control screening for background binding to Fc was performed in parallel (grey bars).

a third selection strategy performed in parallel, using four rounds of solid-phase selection with CD25–Fc-coated ELISA wells as solid support, indicated no positive binders of CD25. Instead 30% of the clones in the solid-phase selection round 4 were observed to be positive for binding to the Fc part of the protein in ELISA screening, despite efforts with negative selections before each round to avoid these unwanted binders (results not shown).

DNA sequencing was performed on 101 ELISA-positive clones, 88 from the anti-IgG Affibody® (Z_2) bead selection and 13 from the selection using Protein A beads, identifying 16 unique phagemid inserts, occurring from once to 56 times (Figure 3A). Sequence cluster analysis [46] revealed that some sequence similarities between groups of the Affibody® molecule's amino acid sequences could be observed, whereas others showed very few homologous residues (Figure 3B). Principally, two main clusters with different sequences could be observed, one containing the dominating sequence $Z_{CD25:2015}$ (occurring 56 times) and one containing, among others, the sequence $Z_{CD25:2020}$ (occurring four times). Five different Affibody® variants from the CD25 selection, representing both sequence groups, were chosen for further characterization.

Production of the generated Affibody® proteins

The five different Affibody® molecules ($Z_{CD25:2015}$, $Z_{CD25:2018}$, $Z_{CD25:2020}$, $Z_{CD25:2021}$ and $Z_{CD25:2022}$) from the CD25 selection were chosen for further analysis and subcloned for expression in *E. coli* as monomers. Moreover, head-to-tail dimeric constructs were generated for two of the CD25-binding Affibody® molecules, $Z_{CD25:2015}$ and $Z_{CD25:2020}$. All CD25-binding Affibody® molecules were expressed fused

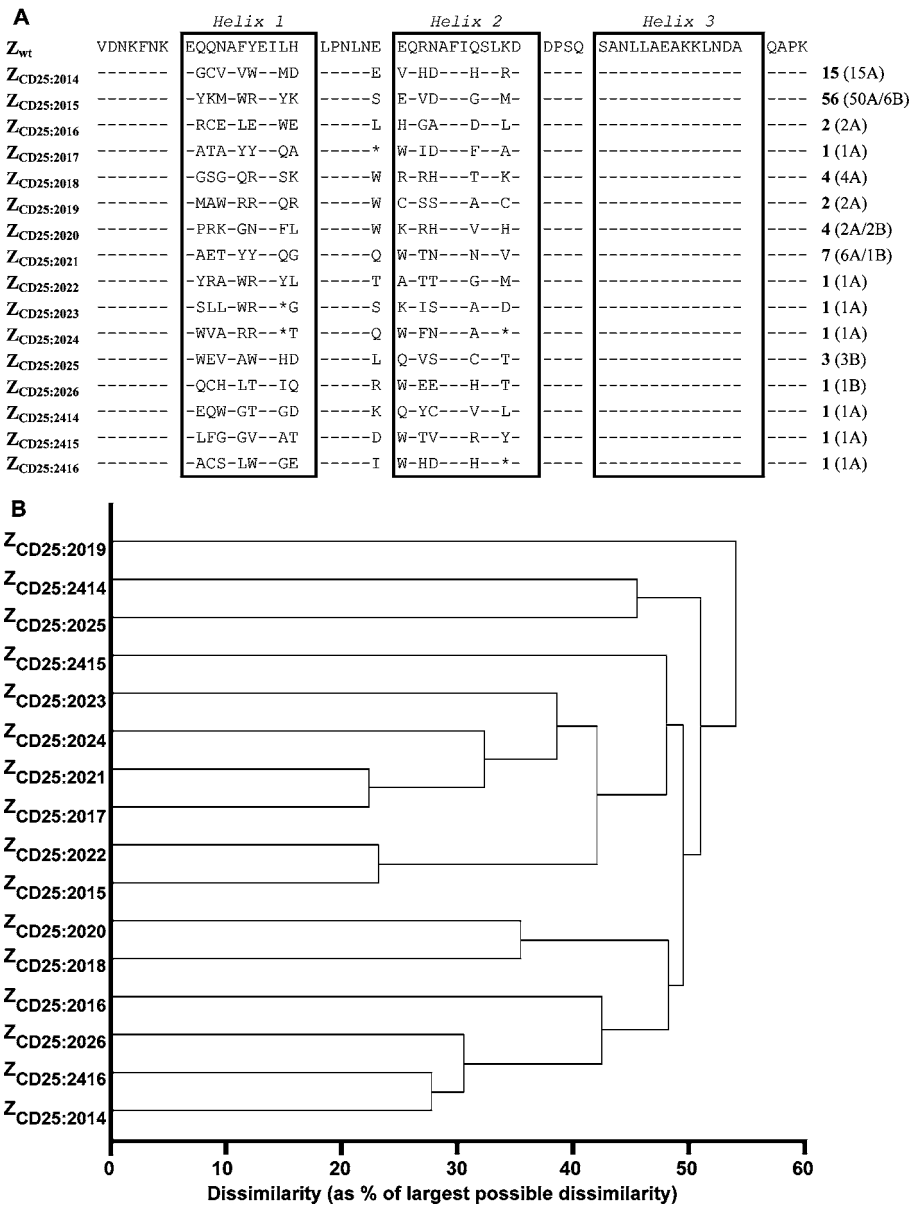

Figure 3 Affibody® molecules selected in the CD25 phage-display selections

(**A**) Amino acid sequence corresponding to wild-type (wt) Z aligned to amino acid sequences of different Affibody® molecules selected against human CD25. The 13 randomized amino acid residuals are presented for the Affibody® molecules and horizontal bars indicate amino acid identities. The three α-helices in the Z scaffold are boxed. The values on the extreme right represent the number of occurrences for each variant revealed upon DNA sequencing of 101 clones. The first value represents the total number of clones and in parentheses is the number of clones from the selection with capture on Z_2-coated beads (selection A) and clones from the selection with capture on Protein A beads (selection B). (**B**) Sequence clustering. The Affibody® molecules were clustered using an average-link hierarchical clustering method, and the result is illustrated in a dendrogram.

to an N-terminal His_6 peptide tag, and the head-to-tail dimers were, in addition, expressed both with and without a unique C-terminal cysteine residue for directed labelling and coupling. The Affibody® proteins were expressed intracellularly in *E. coli* and purified on IMAC columns. Estimations from A_{280} measurements demonstrated high yields of pure protein, approx. 50–100 mg/litre of cell culture medium for monomers and approx. 30–45 mg/litre of cell culture medium for the dimers. The purified proteins were observed as distinct bands of the expected molecular mass when analysed by SDS/PAGE, indicating pure and stable Affibody® molecules (results not shown).

Biosensor binding studies of selected binders

The binding properties of the five candidate Affibody® molecules ($Z_{CD25:2015}$, $Z_{CD25:2018}$, $Z_{CD25:2020}$, $Z_{CD25:2021}$ and $Z_{CD25:2022}$) to CD25 were investigated by surface plasmon resonance biosensor technology using a Biacore® instrument, by subsequently injecting the monomeric ligands over an amine-coupled CD25 surface. The biosensor analysis revealed that four out of five Affibody® molecules ($Z_{CD25:2015}$, $Z_{CD25:2018}$ $Z_{CD25:2020}$ and $Z_{CD25:2022}$) demonstrated significant binding capacity to CD25, whereas the Affibody® molecule $Z_{CD25:2021}$ showed considerably weaker binding in this experiment (results not shown). As expected, none of the Affibody® proteins showed any binding to human polyclonal Fc or to an irrelevant Fc-fused control protein, confirming that no cross-reactivity towards the Fc-part of the target protein CD25–Fc occurred in the phage display selection (results not shown). Besides, no differences in Affibody® binding capacity to a CD25-immobilized surface and a surface coupled with CD25–Fc fusion protein, was observed (results not shown). To assure that coupling of CD25 with amine chemistry did not interfere with the interaction between CD25 and the Affibody® ligands, CD25 fused to human Fc (CD25-Fc) was injected over a Protein A surface, giving a directed immobilization of CD25 due to the Fc-Protein A interaction. Injections of the CD25-binding Affibody® ligands over this CD25–Fc–Protein A surface gave in principle identically shaped binding curves as injections over the amine coupled surface and it could thereby be concluded that the Affibody®-binding region of CD25 and presumably also the functionality of CD25 had not been altered by the amine coupling (results not shown).

The two most promising binders from the initial Biacore® screening, $Z_{CD25:2015}$ and $Z_{CD25:2020}$, were selected for further binding analysis. First, the monomeric Affibody® molecules (His_6-$Z_{CD25:2015}$ and His_6-$Z_{CD25:2020}$) were subjected to kinetic analysis by injection at different concentrations over a CD25 biosensor surface. The resulting sensorgrams (results for $Z_{CD25:2015}$ not shown; for $Z_{CD25:2020}$, see Figure 4A) were analysed with the BIAevaluation 3.2 software (Biacore), assuming 1:1 interactions, and the dissociation equilibrium constants (K_D) could be estimated to be 240 nM for $Z_{CD25:2015}$ and 130 nM for $Z_{CD25:2020}$ by steady-state determinations.

In order to determine avidity, head-to-tail Affibody® dimers were constructed for the CD25-binding Affibody® ligands $Z_{CD25:2015}$ and $Z_{CD25:2020}$. The difference in binding profile due to avidity could clearly be demonstrated by injecting the same concentration of dimers and monomers over a CD25-coupled biosensor surface (Figure 4B). Construction of head-to-tail Affibody® dimers can generally be expected to gain an approx. 5–10-fold improvement in apparent affinity due to avidity effects compared with the corresponding monomeric protein. As expected, the bivalent constructs indeed demonstrated significantly slower dissociation (Figure 4B). However, it was not possible to assign a numeric K_D value, since a 1:1 interaction model would be inappropriate. Nevertheless, the interaction between CD25 and the Affibody® ligands was also compared with the binding profile of the natural ligand, IL-2, in the same manner (Figure 4B). Interestingly, IL-2 is known to bind CD25 with an affinity in the range of 10–30 nM

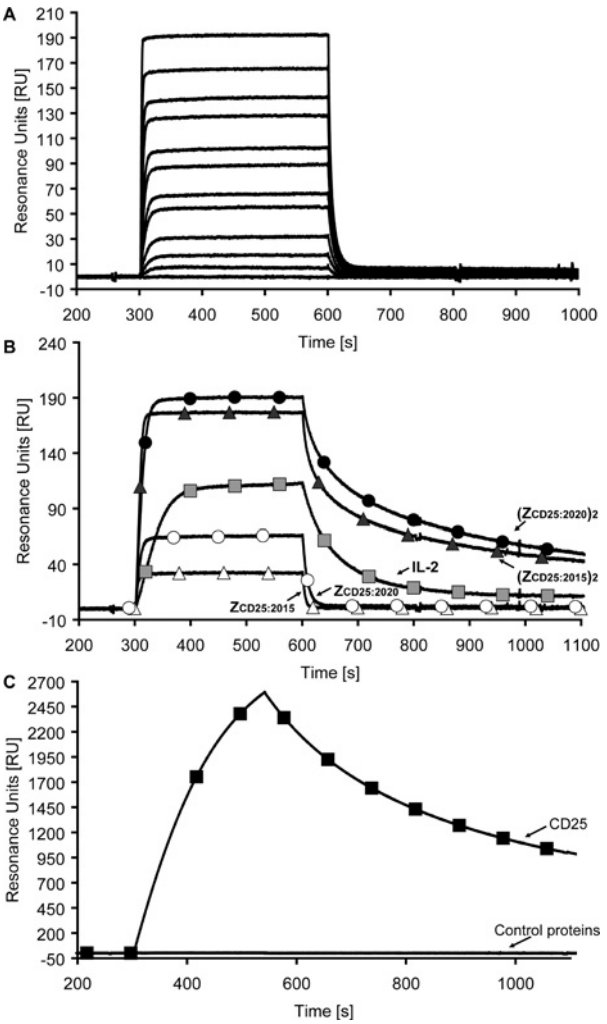

Figure 4 Biacore® binding studies

(**A**) Kinetic analysis of the monomeric anti-CD25 Affibody® molecule $Z_{CD25:2020}$. Sensorgrams were obtained after injection of purified His_6-$Z_{CD25:2020}$ over an amine-coupled CD25 surface at selected concentrations: 0, 5, 10, 20, 40, 50, 80, 100, 160, 200, 320 and 640 nM. (**B**) Comparison of the CD25-binding Affibody® molecules $Z_{CD25:2015}$ and $Z_{CD25:2020}$, as monomeric and dimeric proteins, with the natural ligand, IL-2. The proteins His_6-$Z_{CD25:2015}$, His_6-$Z_{CD25:2020}$, His_6-$(Z_{CD25:2015})_2$, His_6-$(Z_{CD25:2020})_2$ and IL-2 were separately injected over an amine-coupled CD25 surface at a concentration of 50 nM. (**C**) Biacore® specificity analysis. Nine control proteins and CD25–Fc were separately injected over a thiol-coupled anti-CD25 Affibody® His_6-$(Z_{CD25:2020})_2$-Cys surface at a concentration of 3 μg/ml. Sensorgrams are shown for the following proteins: CD25-Fc (■) and, sensorgrams illustrated without symbols, HSA, IgG, Fc, haemopexin, transferrin, fibrinogen, IgA, complement C4 and streptavidin.

[6] and, when the dissociation phase of the interaction was analysed, the IL-2 binding curve seems to be comparable with the binding curves for the dimeric Affibody® molecules (Figure 4B).

Biosensor determination of Affibody® ligand specificity for CD25

Biosensor technology was used for studying the specificity of the candidate CD25-binding Affibody® molecules $Z_{CD25:2015}$ and $Z_{CD25:2020}$. The Affibody® dimers [His_6-($Z_{CD25:2015}$)$_2$-Cys and His_6-($Z_{CD25:2020}$)$_2$-Cys] were immobilized specifically in a directed manner to two Biacore® biosensor surfaces using the C-terminal cysteine residues. It is to be noted that, having a bivalent ligand immobilized on the Biacore chip, there will be no affinity contributions through avidity effects. Seven highly abundant human serum proteins, CD25, human polyclonal Fc and streptavidin, were separately injected over the Affibody® surfaces. Both CD25-binding Affibody® molecules proved to have a strikingly high specificity for CD25, and only very low background binding could be observed for the nine control proteins (Figure 4C).

Moreover, the CD25-binding Affibody® molecules ($Z_{CD25:2015}$ and $Z_{CD25:2020}$) showed high specificity towards the human variant of CD25 compared with the mouse variant, with nearly a 100-fold decrease in biosensor response when mouse CD25 was studied (results not shown). This was not surprising, since the homology in amino acid sequence between the mouse and human extracellular domain of CD25 is only 58%. Hence, these results indicated that the Affibody® molecules interact with a human CD25 epitope with some distinct differences from the mouse homologue.

Epitope mapping by biosensor analysis of competitive binding

The two most promising CD25-binding Affibody® molecules, namely $Z_{CD25:2015}$ and $Z_{CD25:2020}$, represented two clusters with sequence dissimilarities, as visualized in Figure 3. Thus it would be of interest to evaluate whether the Affibody® ligands bound to the same region of CD25 despite the lack of conserved residues between the two Affibody® molecules. Therefore recombinant CD25–Fc was mixed with different concentrations of the Affibody® molecule His_6-($Z_{CD25:2015}$)$_2$ and the samples were separately injected over a Biacore® biosensor surface coupled with the Affibody® molecule His_6-($Z_{CD25:2020}$)$_2$-Cys. Despite the lack of obvious similarities in amino acid residues recruited in the varied positions, this experiment clearly showed that the binding of CD25 to $Z_{CD25:2020}$ was efficiently blocked by the Affibody® molecule $Z_{CD25:2015}$, strongly suggesting that the two Affibody® molecules recognize the same, or overlapping, epitopes on CD25 (Figure 5A).

The binding of the ligand IL-2 to CD25 (IL-2Rα) is a well-characterized interaction of clinical importance.

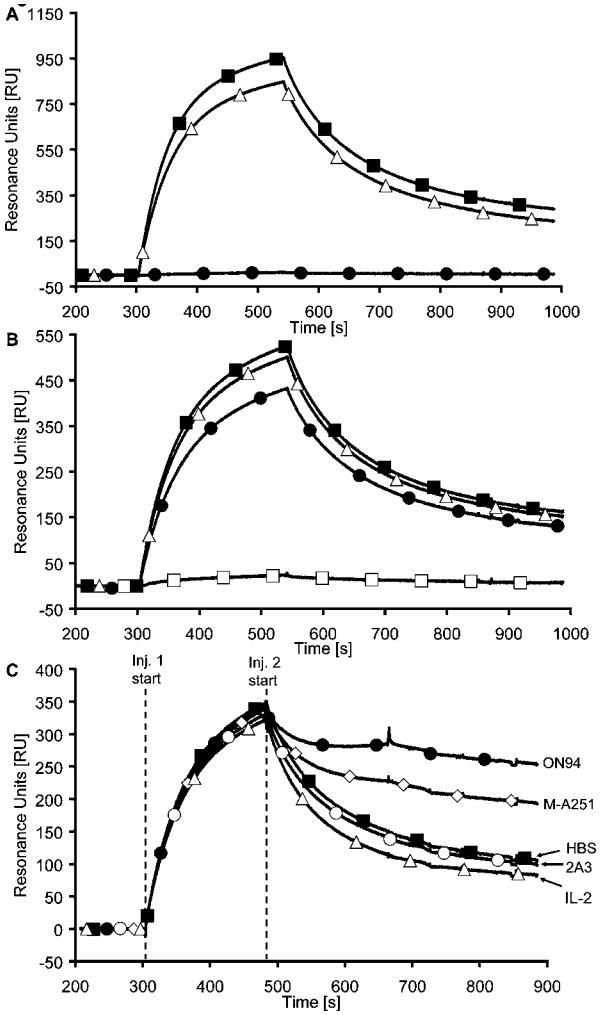

Figure 5 Biacore® competition studies

(**A**) Competition between the two CD25-binding Affibody® molecules $Z_{CD25:2015}$ and $Z_{CD25:2020}$. Equal amounts of CD25–Fc (100 nM) was mixed with 0 (■), 10 (△) or 100 nM (●) His_6-($Z_{CD25:2015}$)$_2$ and separately injected over a thiol-coupled anti-CD25 Affibody® His_6-($Z_{CD25:2020}$)$_2$-Cys surface. (**B**) Competition between the CD25-binding Affibody® molecule $Z_{CD25:2020}$ and the natural ligand IL-2. Equal amounts of CD25-Fc (50 nM) were mixed with 0 (■), 5 (△), 50 (●) or 500 nM (□) IL-2 and separately injected over a thiol-coupled anti-CD25 Affibody® His_6-($Z_{CD25:2020}$)$_2$-Cys surface. (**C**) Competition between the CD25-binding Affibody® molecule $Z_{CD25:2020}$ and mAbs. CD25–Fc was injected over a thiol-coupled anti-CD25 Affibody® His_6-($Z_{CD25:2020}$)$_2$-Cys surface, directly followed by an injection of the mAb using the Biacore® command coinject. Three mAbs were studied: ON94 (●) and MA-251 (◇) with no IL-2 blocking capacity and 2A3 (○) binding to the Tac epitope blocking IL-2 binding. HBS buffer (■) was injected as a negative control and IL-2 (△) as a positive control.

It was therefore natural to investigate whether the Affibody® molecules and the natural ligand IL-2 recognize overlapping epitopes. The experimental design was similar to the competition analysis of the two different Affibody® molecules above. The same concentration of CD25–Fc was mixed with different concentrations of IL-2 and separately

injected over a biosensor surface coupled with the $Z_{CD25:2020}$ Affibody® molecule. A clear IL-2-dose-dependent blocking of the interaction between CD25 and Affibody® was observed (Figure 5B), indicating that the Affibody® molecule and IL-2 compete for the same binding site on CD25. To further confirm these results, a different approach for competitive binding in Biacore® was performed, using mAbs with known binding sites. CD25–Fc and the different mAbs were subsequently injected over the $Z_{CD25:2020}$ Affibody® flow-cell surface using co-injection, two closely followed injections being carried out. If the mAb epitope was available after binding of CD25 to the Affibody® surface in the first injection, the mAb will be able to bind when it is injected in the second injection, giving a characteristic binding shape in the sensorgram compared with the normal dissociation. The Affibody® molecule showed no competitive binding for overlapping epitopes with the mAb ON94, binding somewhere in the region of amino acids 3–104 or to the mAb M-A251, binding to the epitope referred to as 'epitope B' not overlapping with the IL-2 site (Figure 5C). The Affibody® molecule did, however, demonstrate strong competition with the mAb 2A3 known to compete with IL-2 for binding to the Tac epitope, also referred to as 'epitope A' (Figure 5C). As expected, clear competition was also shown for the control IL-2. Hence, these results supported the results from the initial biosensor competition studies, suggesting that the CD25-binding Affibody® molecule interacts with the CD25 Tac epitope (epitope A), overlapping the binding site of the natural ligand IL-2.

Immunofluorescence microscopy

Binding of the Affibody® molecules to native CD25 on cells were confirmed by fluorescence microscopy. Binding to both the human IL-2-dependent cell line NK92 and binding to primary $CD25^+$ T-cells ($CD4^+$ $CD25^+$ PBMCs) isolated from healthy blood donors were studied by immunofluorescence. The fixed cells were stained with the OG-conjugated Affibody® molecule $Z_{CD25:2020}$, and a clear staining of both the NK92 cells and the $CD4^+$ $CD25^+$ PBMCs (Figure 6) was displayed. An irrelevant control Affibody® molecule demonstrated no background staining of the cells (results not shown). In addition, no staining of $CD25^-$cells ($CD4^+$ $CD25^-$) was observed with the CD25-binding Affibody® molecule $Z_{CD25:2020}$ (Figure 6). The cells were also stained with DAPI (4′,6-diamidino-2-phenylindole) to visualize the cell nuclei.

Flow-cytometric analysis of CD25 binding on cells

The CD25-binding Affibody® molecule $Z_{CD25:2020}$ was subjected to flow-cytometric analysis in order to confirm binding to native CD25 expressed on the cell surface of human cells. First, the binding of a dimeric Affibody® molecule, site-specifically labelled with OG, to the IL-2-dependent human cell line NK92 (Figure 7A) and primary $CD25^+$ T-cells ($CD4^+$ $CD25^+$ PBMCs; Figure 7B) was analysed. Secondly, binding of the monomeric Affibody® molecule to PHA-stimulated PBMCs (PHA blasts; Figure 8) was analysed, utilizing detection with goat anti-Affibody® antibodies and Alexa 647®-conjugated anti-goat antibodies. CD25 expression on the different cell types were confirmed, with CD25-specific antibodies showing expected CD25 expression levels on the cells (results not shown). The CD25-binding Affibody® molecule demonstrated clear binding to all three CD25-expressing cells (Figures 7 and 8) in the two different experimental set-ups. No non-specific binding to $CD25^-$ cells ($CD4^+$ $CD25^-$ PBMC) was detected (Figure 7C), and the negative control Affibody® molecule showed no binding to the CD25-positive cells. This indicates that the CD25-binding Affibody® molecule binds specifically to CD25 and recognizes native CD25 expressed on the surface of human cells.

Discussion

In the present study, phage-display technology was used to successfully select novel Affibody® molecules that selectively bind to the IL-2Rα subunit (CD25). The selection strategy involved using the target protein CD25 fused to the Fc part of human IgG. By taking advantage of the interaction between Fc and Protein A, phage–target complexes in the selection could be captured on magnetic beads coated with different forms of Protein A, thus circumventing the risk of altering important binding sites with modifications such as biotinylation of the target. In our selection, this strategy also proved to be more successful in generating binders than did the conventional coating of CD25 to a plastic surface. Furthermore, the selection using the dimeric Protein A variant Z_2 site-specifically biotinylated via the C-terminal cysteine residue and immobilized to streptavidin beads, seemed more successful than using paramagnetic beads precoated with native pentavalent Protein A as the solid support.

Four Affibody® molecules from the CD25 phage-display selection, namely $Z_{CD25:2015}$, $Z_{CD25:2018}$, $Z_{CD25:2020}$ and $Z_{CD25:2022}$, out of five chosen for detailed characterization, demonstrated significant binding to CD25, whereas the fifth ($Z_{CD25:2021}$) showed considerably weaker binding in biosensor studies. When the amino acid sequence similarities between the selected Affibody® molecules was analysed, two similarity clusters could be suggested with virtually no homologies between the two groups. Interestingly, the two top candidate binders, $Z_{CD25:2015}$ and $Z_{CD25:2020}$, representing these two sequence clusters, were found to compete in their binding to CD25 in biosensor analysis, indicating overlapping

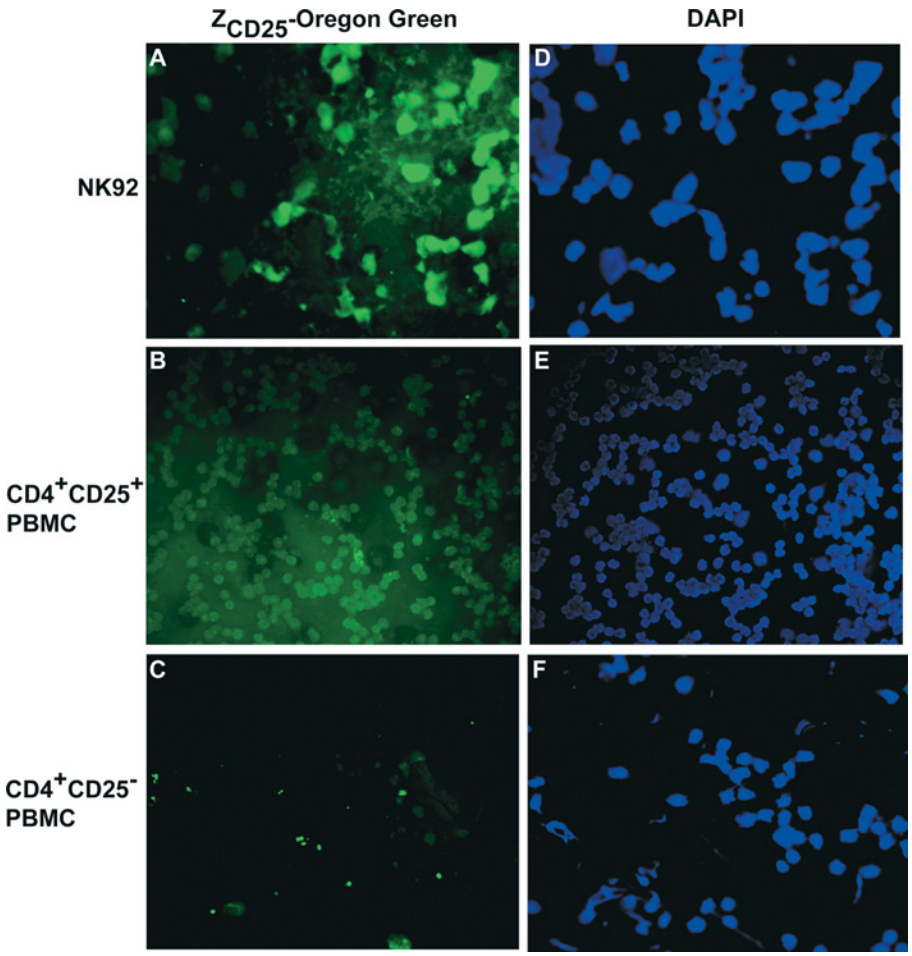

Figure 6 Immunofluorescence-microscopic image of the human IL-2-dependent cell line NK92 and isolated $CD25^+$ PMBCs

$CD25^-$ PBMCs were used as a negative control. (**A**)–(**C**) show staining with the Affibody® molecule His_6-$(Z_{CD25:2020})_2$ directly labelled with OG, and (**D**)–(**F**) show DAPI-labelled nuclei.

binding sites, despite their differences in amino acid residues. Although both CD25-binding Affibody® molecules demonstrated similar binding properties in biosensor studies, it cannot be concluded from the present results whether the Affibody® molecules bind overlapping binding sites or identical epitopes. Furthermore, both Affibody® molecules were found to exhibit equally strikingly high specificity towards CD25, showing, in principle, no binding to the control proteins. In addition, the Affibody® molecules were observed to be specific for human CD25 and showed considerably weaker binding to murine CD25.

Biosensor kinetic analysis revealed that the CD25-binder $Z_{CD25:2020}$ had a twofold higher affinity for CD25 compared with the binder $Z_{CD25:2015}$, and it was therefore selected as the preferred binder for future studies. The fact that the most abundant Affibody® molecule in the selection, in this case $Z_{CD25:2015}$, did not exhibit the highest apparent affinity, is not unusual in selections [43], and it could possibly be explained by slight differences in expression levels contributing to the convergence in the selection. However, no obvious differences between the two Affibody® molecules in expression and stability could be observed.

In an epitope-mapping effort using a competitive biosensor set-up, the CD25-binding Affibody® molecules were demonstrated to recognize the same, or at least an overlapping, CD25 binding site as the mAb 2A3, i.e. the Tac epitope. The mAb 2A3 blocks binding of the natural ligand IL-2 and the Affibody® molecules showed no competition with antibodies towards other epitopes without IL-2-blocking capacity. In addition, IL-2 was found to block the binding of CD25 to the Affibody® molecules in a dose-dependent manner, thus confirming that the Affibody® molecules have overlapping epitopes with IL-2 and the anti-CD25 antibodies binding the Tac epitope. Interestingly, this also implies that the Affibody® molecules should interact with

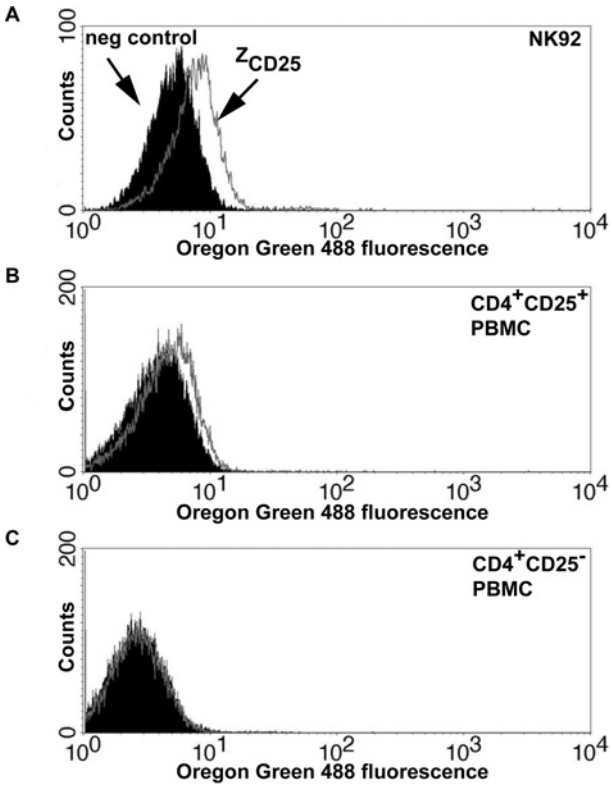

Figure 7 Flow-cytometric analysis of the binding of the fluorescently labelled dimeric CD25-binding Affibody® molecule $(Z_{CD25:2020})_2$ to native CD25 expressed on the cell surface of NK92 cells (A), CD25+ PBMCs (B) and the negative-control cells ($CD25^-$ PMBCs) (C)

The result from the CD25-binding Affibody® molecule (white area) can be compared with the result from the negative-control Affibody® molecule (black area). The Affibody® molecules were labelled directly with OG on a unique C-terminal cysteine residue.

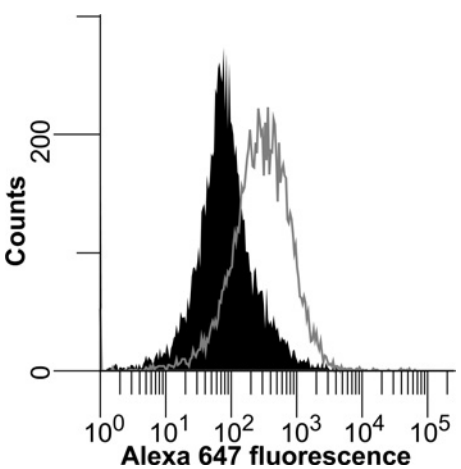

Figure 8 Flow-cytometric analysis of binding of the monomeric CD25-binding Affibody® molecule $Z_{CD25:2020}$ to PHA-activated PBMCs expressing high levels of CD25

The cells were stained with His_6-$Z_{CD25:2020}$ (white area) or the negative-control Affibody® (black area) and binding was detected with goat anti-Affibody® antibodies and Alexa 647®-conjugated anti-goat antibodies.

the same binding site as the chimaeric therapeutic antibody Basiliximab and the corresponding humanized antibody Daclizumab. The epitope for Basiliximab and Draclizumab have recently been suggested to comprise the amino acid residues 116–122 in the CD25 domain 2 [57]. These results can be compared with the crystal structure of IL-2 in complex with CD25, since the binding site of Basiliximab and IL-2 overlap. The interaction interface between IL-2 and CD25 comprises 21 residues in CD25 located in domain 1 (amino acids 25–43) and 2 (amino acids 118–120) [4]. The IL-2-blocking antibodies most probably impair the interaction between the receptor and IL-2 by binding to the contact residues 118–120 [57]. These residues could make up part of the binding site for the CD25 Affibody® molecules, but other residues might be equally or more important, since the Affibody® molecules bind weakly to murine CD25 where these residues are conserved.

The epitope mapping of the Affibody® ligands to the IL-2 binding site strongly indicated that the Affibody® molecules should be able to interact with native CD25 expressed on the cell surface of active T-cells. Indeed, a clear binding of $Z_{CD25:2020}$ to CD25-positive PBMCs and a human IL-2-dependent cell line could be visualized in immunofluorescence microscopy. This was despite presumed difficulties in fluorescence detection caused by the rather low number of CD25 receptors normally expressed, even on overexpressing cells, namely 10 000–30 000 [12], the affinity of the Affibody® molecule, together with the possibility of IL-2 present blocking the receptor. In addition, we could also detect clear shifts on flow-cytometric analysis for the anti-CD25 Affibody® molecule compared with an irrelevant Affibody® molecule when primary $CD25^+$ PBMCs, human NK92 cells and PHA-activated PBMCs (PHA blasts) expressing CD25 were analysed. The flow-cytometric analysis was performed with two different experimental set-ups and on both primary cells and a CD25-expressing cell line. Both cases gave the same result, and no binding of the Affibody® was detected on $CD25^-$ cells. Hence these results confirm specific binding of the Affibody® molecule to native CD25 on cells, and higher fluorescence intensity in immunofluorescence microscopy and flow cytometry could be expected with an improvement in affinity.

Affibody® molecules targeting CD25-expressing cells have a wide variety of different very promising future applications. CD25 is in many aspects a unique target both for immunotherapy and medical imaging. The very low expression in resting immune cells gives the rare possibility of a directed targeting of the aimed cells without risking background binding to other cells. CD25 and the IL-2 cytokine system have been intensely studied over the years, resulting in a major collected knowledge about its functionality in the immune system and the large

number of serious disease conditions exhibiting CD25 overexpression. By directing the therapy with molecular targeting to the cells involved in the disease instead of systemic treatment, therapy could be improved and reactions caused by unspecific treatment could, to a greater extent, be avoided. In therapeutics, CD25-binding Affibody® molecules could be used for targeting CD25-expressing cells in the prevention of organ allograft rejections in transplantations, treatment of autoimmune diseases and treatment of CD25-expressing-T-cell malignancies. In all three cases the therapeutic effect could either be induced by blocking the interaction of the natural ligand IL-2 and the receptor, thereby restraining T-cell activation and proliferation, or by delivering a therapeutic effector group as, for example a radionuclide or a cytotoxic conjugate, to the target cells. The Affibody® molecules could also be considered for apheresis in severe T-cell leukaemia or autoimmune disease to remove the CD25-overexpressing cells by extracorporeal capture to improve the clinical status of the patients. Affibody® molecules can conveniently be produced in different formats, and the possibility of utilizing a C-terminal cysteine residue gives the possibility of directed immobilization of the Affibody® molecules to an affinity resin or directed coupling of therapeutic compounds without affecting the binding surface.

CD25-binding Affibody® molecules might be used in diagnostic applications to detect soluble CD25 in circulation. This would enable further investigation of the possible correlation of serum levels of soluble CD25 with disease activity in autoimmune conditions, and the possible use of soluble CD25 as a biomarker for response to therapeutic treatment [7].

Medical imaging is another application in the diagnostics field where Affibody® molecules are very well suited. Affibody® molecules have recently shown promising results in imaging of malignant tumours by targeting radionuclide to tumour-specific antigens [47–50]. The small size of the Affibody® molecules gives the molecules the relatively short half-life that is suitable for imaging products. Affibody® molecules have shown impressively high selectivity for their target, and it has been demonstrated that very-high-affinity binders can be obtained (down to the picomolar range of K_D). In the case of *in vivo* medical imaging of $CD25^+$ cells, two main areas of interest can be envisioned, i.e. imaging of inflammation in autoimmune disease and imaging of infiltration of active immune cells in solid tumours. Imaging with the present Affibody® molecules binding to CD25 or a second-generation affinity-matured binder interacting with the same epitope, could be complicated by the competition with IL-2 for the same binding site. However, the very short half-life of IL-2 (5–7 min) and the relatively low affinity of IL-2 for CD25 alone could presumably compensate for this. Visualization of active T-cells by *in vivo* imaging could facilitate monitoring the diseases in relation to clinical outcome, which could eventually lead to our gaining more knowledge about the role of active T-cells in disease and with the possibility of more personalized biotherapy and improved treatment for the patients.

High affinity of the targeting agent is crucial in both therapeutic and imaging applications. One way of improving the affinity, namely decreasing the K_D, is to convert a monomeric ligand into a dimeric one in order to gain avidity effects. With Affibody® molecules this has previously been demonstrated to result in a 5–10-fold increase in apparent affinity. Moreover, the affinity of Affibody® molecules can by improved by a straightforward affinity-maturation strategy. This strategy has in several cases proved to be very effective in generating high-affinity binders [46], and affinity maturation would naturally be an important step towards therapeutic and imaging applications for the CD25-binding Affibody® molecules.

In conclusion, the novel Affibody® molecules binding CD25 (IL-2Rα subunit) have demonstrated significant binding to recombinant CD25 and to native CD25 expressed on cells. We found that the Affibody® molecules have overlapping binding sites with the natural ligand IL-2, a feature that would possibly enable future therapeutic applications by blocking the IL-2 interaction. We believe that the CD25-binding Affibody® molecules might have a potential as prospective therapeutic and medical-imaging agents. The Affibody® molecules offer many advantages compared with, for example, mAbs, owing to their small size, robustness and efficient bacterial expression or chemical synthesis, giving low production costs. It would be of great interest to further evaluate the CD25-binding Affibody® molecules, and an affinity-maturation effort should perhaps be considered in order to gain a high-affinity second-generation binder that could be investigated in *in vivo* experiments.

Acknowledgments

We thank Dr Mikaela Friedman (Department of Molecular Biotechnology, Royal Institute of Technology, Stockholm, Sweden), Dr Andreas Jonsson (Affibody® AB, Bromma, Sweden) and Professor Pavel Pisa (Karolinska Institutet, Stockholm, Sweden) for valuable advice. We thank Dr Siraç Dilber for kindly providing the NK92 cells. Affibody® is a trademark of Affibody AB, Bromma, Sweden, and is registered in Sweden, Europe and the U.S.A.

References

1 Wang, X., Rickert, M. and Garcia, K. C. (2005) Science **310**, 1159–1163

2 Nelson, B. H., Lord, J. D. and Greenberg, P. D. (1994) Nature **369**, 333–336
3 Gaffen, S. L. (2001) Cytokine **14**, 63–77
4 Rickert, M., Wang, X., Boulanger, M. J., Goriatcheva, N. and Garcia, K. C. (2005) Science **308**, 1477–1480
5 Wang, H. M. and Smith, K. A. (1987) J. Exp. Med. **166**, 1055–1069
6 Liparoto, S. F. and Ciardelli, T. L. (1999) J. Mol. Recognit. **12**, 316–321
7 Morris, J. C. and Waldmann, T. A. (2000) Ann. Rheum. Dis. **59**, Suppl. 1, i109–i114
8 Frey, O. and Brauer, R. (2006) Arch. Immunol. Ther. Exp. (Warszawa) **54**, 33–43
9 Beyer, M. and Schultze, J. L. (2006) Blood **108**, 804–811
10 Dejaco, C., Duftner, C., Grubeck-Loebenstein, B. and Schirmer, M. (2006) Immunology **117**, 289–300
11 Waldmann, T. A. (2007) Oncogene **26**, 3699–3703
12 Waldmann, T. A. (2007) J. Clin. Immunol. **27**, 1–18
13 Holliger, P. and Hudson, P. J. (2005) Nat. Biotechnol. **23**, 1126–1136
14 Winter, G., Griffiths, A. D., Hawkins, R. E. and Hoogenboom, H. R. (1994) Annu. Rev. Immunol. **12**, 433–455
15 Davies, J. and Riechmann, L. (1996) Protein Eng. **9**, 531–537
16 Bird, R. E., Hardman, K. D., Jacobson, J. W., Johnson, S., Kaufman, B. M., Lee, S. M., Lee, T., Pope, S. H., Riordan, G. S. and Whitlow, M. (1988) Science **242**, 423–426
17 Huston, J. S., Levinson, D., Mudgett-Hunter, M., Tai, M. S., Novotny, J., Margolies, M. N., Ridge, R. J., Bruccoleri, R. E., Haber, E., Crea, R. et al. (1988) Proc. Natl. Acad. Sci. U.S.A. **85**, 5879–5883
18 Holliger, P., Prospero, T. and Winter, G. (1993) Proc. Natl. Acad. Sci. U.S.A. **90**, 6444–6448
19 Desmyter, A., Spinelli, S., Payan, F., Lauwereys, M., Wyns, L., Muyldermans, S. and Cambillau, C. (2002) J. Biol. Chem. **277**, 23645–23650
20 Holt, L. J., Herring, C., Jespers, L. S., Woolven, B. P. and Tomlinson, I. M. (2003) Trends Biotechnol. **21**, 484–490
21 Binz, H. K., Amstutz, P. and Plückthun, A. (2005) Nat. Biotechnol. **23**, 1257–1268
22 Hey, T., Fiedler, E., Rudolph, R. and Fiedler, M. (2005) Trends Biotechnol. **23**, 514–522
23 Nygren, P. Å. and Skerra, A. (2004) J. Immunol. Methods **290**, 3–28
24 Nygren, P. Å. and Uhlén, M. (1997) Curr. Opin. Struct. Biol. **7**, 463–469
25 Skerra, A. (2000) J. Mol. Recognit. **13**, 167–187
26 Koide, A., Abbatiello, S., Rothgery, L. and Koide, S. (2002) Proc. Natl. Acad. Sci. U.S.A. **99**, 1253–1258
27 Xu, L., Aha, P., Gu, K., Kuimelis, R. G., Kurz, M., Lam, T., Lim, A. C., Liu, H., Lohse, P. A., Sun, L. et al. (2002) Chem. Biol. **9**, 933–942
28 Skerra, A. (2000) Biochim. Biophys. Acta **1482**, 337–350
29 Binz, H. K., Amstutz, P., Kohl, A., Stumpp, M. T., Briand, C., Forrer, P., Grutter, M. G. and Plückthun, A. (2004) Nat. Biotechnol. **22**, 575–582
30 Schneider, S., Buchert, M., Georgiev, O., Catimel, B., Halford, M., Stacker, S. A., Baechi, T., Moelling, K. and Hovens, C. M. (1999) Nat. Biotechnol. **17**, 170–175
31 Nord, K., Gunneriusson, E., Ringdahl, J., Ståhl, S., Uhlén, M. and Nygren, P. Å. (1997) Nat. Biotechnol. **15**, 772–777
32 Nord, K., Nilsson, J., Nilsson, B., Uhlén, M. and Nygren, P. Å. (1995) Protein Eng. **8**, 601–608
33 Nilsson, B., Moks, T., Jansson, B., Abrahmsén, L., Elmblad, A., Holmgren, E., Henrichson, C., Jones, T. A. and Uhlén, M. (1987) Protein Eng. **1**, 107–113
34 Gräslund, S., Eklund, M., Falk, R., Uhlén, M., Nygren, P. Å. and Ståhl, S. (2002) J. Biotechnol. **99**, 41–50
35 Nord, K., Gunneriusson, E., Uhlén, M. and Nygren, P. Å. (2000) J. Biotechnol. **80**, 45–54
36 Nord, K., Nord, O., Uhlén, M., Kelley, B., Ljungqvist, C. and Nygren, P. Å. (2001) Eur. J. Biochem. **268**, 4269–4277
37 Andersson, M., Rönnmark, J., Areström, I., Nygren, P. Å. and Ahlborg, N. (2003) J. Immunol. Methods **283**, 225–234
38 Karlström, A. and Nygren, P. Å. (2001) Anal. Biochem. **295**, 22–30
39 Renberg, B., Shiroyama, I., Engfeldt, T., Nygren, P. K. and Karlström, A. E. (2005) Anal. Biochem. **341**, 334–343
40 Rönnmark, J., Hansson, M., Nguyen, T., Uhlén, M., Robert, A., Ståhl, S. and Nygren, P. Å. (2002) J. Immunol. Methods **261**, 199–211
41 Sandström, K., Xu, Z., Forsberg, G. and Nygren, P. Å. (2003) Protein Eng. **16**, 691–697
42 Grönwall, C., Sjöberg, A., Ramström, M., Höiden-Guthenberg, I., Hober, S., Jonasson, P. and Ståhl, S. (2007) Biotechnol. J. **2**, 1389–1398
43 Friedman, M., Nordberg, E., Höidén-Guthenberg, I., Brismar, H., Adams, G. P., Nilsson, F. Y., Carlsson, J. and Ståhl, S. (2007) Protein Eng. Des. Select. **20**, 189–199
44 Steffen, A. C., Wikman, M., Tolmachev, V., Adams, G. P., Nilsson, F. Y., Ståhl, S. and Carlsson, J. (2005) Cancer Biother. Radiopharm. **20**, 239–248
45 Wikman, M., Steffen, A. C., Gunneriusson, E., Tolmachev, V., Adams, G. P., Carlsson, J. and Ståhl, S. (2004) Protein Eng. Des. Select. **17**, 455–462
46 Orlova, A., Magnusson, M., Eriksson, T. L., Nilsson, M., Larsson, B., Höidén-Guthenberg, I., Widström, C., Carlsson, J., Tolmachev, V., Ståhl, S. and Nilsson, F. Y. (2006) Cancer Res. **66**, 4339–4348
47 Nilsson, F. Y. and Tolmachev, V. (2007) Curr. Opin. Drug Discovery Dev. **10**, 167–175
48 Tolmachev, V., Orlova, A., Nilsson, F. Y., Feldwisch, J., Wennborg, A. and Abrahmsén, L. (2007) Expert Opin. Biol. Ther. **7**, 555–568
49 Baum, R. P., Orlova, A., Tolmachev, V. and and Feldwich, J. (2006) Eur. J. Nucl. Med. Mol. Imaging **33**, 91
50 Orlova, A., Tran, T., Widström, C., Engfeldt, T., Eriksson Karlström, A. and Tolmachev, V. (2007) Int. J. Mol. Med. **20**, 397–404

51 Engfeldt, T., Renberg, B., Brumer, H., Nygren, P. Å. and Karlström, A. E. (2005) ChemBiochem **6**, 1043–1050
52 Rüther, U. (1982) Nucleic Acids Res. **10**, 5765–5772
53 Grönwall, C., Jonsson, A., Lindström, S., Gunneriusson, E., Ståhl, S. and Herne, N. (2007) J. Biotechnol. **128**, 162–183
54 Studier, F. W., Rosenberg, A. H., Dunn, J. J. and Dubendorff, J. W. (1990) Methods Enzymol. **185**, 60–89
55 Hansson, M., Ringdahl, J., Robert, A., Power, U., Goetsch, L., Nguyen, T. N., Uhlén, M., Ståhl, S. and Nygren, P. Å. (1999) Immunotechnology **4**, 237–252
56 Ståhl, S., Nilsson, J., Hober, S., Uhlén, M. and Nygren, P. Å. (1999) in Encyclopedia of Bioprocess Technology: Fermentation, Biocatalysis and Bioseparation (Flickinger, M. C. and Drew, S. W., eds.), pp. 49–63, Wiley, New York
57 Binder, M., Vogtle, F. N., Michelfelder, S., Muller, F., Illerhaus, G., Sundararajan, S., Mertelsmann, R. and Trepel, M. (2007) Cancer Res. **67**, 3518–3523

Received 30 November 2007/25 January 2008; accepted 19 February 2008
Published as Immediate Publication 19 February 2008, doi:10.1042/BA20070261